Theoretical Investigation of *N*-Methyl-*N′*-(4-nitrobenzylidene) pyrazine-2-carbohydrazide: Conformational Study, NBO Analysis, Molecular Structure and NMR Spectra

N. Günay[a], Ö. Tamer[b], D. Kuzalic[c], D. Avci[b] and Y. Atalay[b,*]

[a]Beykent University, Department of Health Programmes, Opticianry Programme, İstanbul, Turkey

[b]Sakarya University, Faculty of Arts and Sciences, Department of Physics, 54187, Sakarya, Turkey

[c]Beykent University,Faculty of Enginering, Department of Chemical Enginering, İstanbul, Turkey

(Received April 17, 2014; in final form January 23, 2015)

The crystal structure determination of the methylated pyrazine-2-carbohydrazide derivative, namely *N*-methyl-*N′*-(4-nitrobenzylidene)pyrazine-2-carbohydrazide were optimized to obtain its molecular geometric structure and electronic structures at the Hartree–Fock and density functional theory levels (B3LYP) with 6-311G(d,p) and 6-311++G(d,p) basis sets, using Gaussian 09W programme. The ^{1}H and ^{13}C nuclear magnetic resonance chemical shifts of the title molecule were calculated by using the gauge independent atomic orbital, continuous set of gauge transformations and individual gauges for atoms in molecules methods and were also compared with experimental values. The electronic properties high occupied and low unoccupied molecular orbitals energies were calculated and analyzed. Potential energy surface scan, natural population analysis and Mulliken atomic charges were investigated using theoretical calculations. A detailed molecular picture and intermolecular interactions arising from hyperconjugative interactions and charge delocalization of the molecule were analyzed using natural bond orbital analysis.

DOI: 10.12693/APhysPolA.127.701

PACS: 31.15.A–, 31.15.ae, 31.15.E–, 33.25.+k, 31.50.Bc

1. Introduction

Pyrazine is a symmetrical and heterocyclic aromatic organic compound having two nitrogen atoms in the para-position of the six-membered ring. Ligands containing pyrazine ring are widely studied and their pi-donor properties are interesting [1]. Pyrazine has been paid great attention, because the diazine rings form an important class of compounds presented in several natural and synthetic compounds [2]. Pyrazine derivatives have been widely used in the fields of medicinal chemistry for the skeleton of biologically active sites [3, 4]. Pyrazines and its derivatives constitute an important class of compounds present in several natural flavours and complex organic molecules [5]. In continuation of these studies, the synthesis and antituberculosis activities of a series of methylated pyrazine-2-carbohydrazide derivatives have been studied [6–8]. Pyrazine derivatives are known as an important drugs with analgesic [9], antimicrobial [10], anticancer [11], sodium channel blocker [12], antiviral [13], antihypertensive [14], antiglaucoma [15], antioxidant [16], antidepressant, anxiolytic, neuroprotective [17] and antidiabetic [18] activity. Pyrazine-2-carbohydrazides have been the object of many spectral, structural and theoretical investigations [19–22]. However, to the best of our knowledge, the theoretical investigations for structural, spectroscopic and electronic properties of *N*-methyl-*N′*-(4-nitrobenzylidene) pyrazine-2-carbohydrazide compound have not been performed. So as to eliminate this deficiency, detailed theoretical investigations were carried out concerning the conformational analysis, vibrational frequencies and NMR chemical shifts, bonding features, high occupied molecular orbital (HOMO) and low unoccupied molecular orbital (LUMO) energies.

2. Computational details

The quantum chemical calculations have been performed by using the Hartree–Fock (HF) method and B3 [23] exchange functional combined with the LYP [24] correlation function resulting in the B3LYP density functional method combined with 6-311G(d,p) and 6-311++G(d,p) basis sets. All electronic and structural computations were performed using Gaussian 09W program [25] and Gauss View 5.0 program package [26]. The potential energy surface was studied at the 6-311G(d,p) level. NBO analyses [27] have been performed by the module NBO version 3.1 implemented in Gaussian 09W [25] at the optimization level to determine the partial charge distribution and the bonding characters of the title molecule.

*corresponding author; e-mail: yatalay@sakarya.edu.tr

3. Results and discussion

3.1. Molecular geometry

In order to find the best optimized geometry the geometric parameters of the title compound were optimized using HF and B3LYP methods with 6-311G(d,p) (marked in Tables $A1$) and 6-311++G(d,p) ($A2$) basis sets. The atom numbering scheme for the molecule is shown in Fig. 1a [8]. The optimized geometry of the title molecule performed at B3LYP/6-311++G(d,p) level with atoms numbering is shown in Fig. 1b.

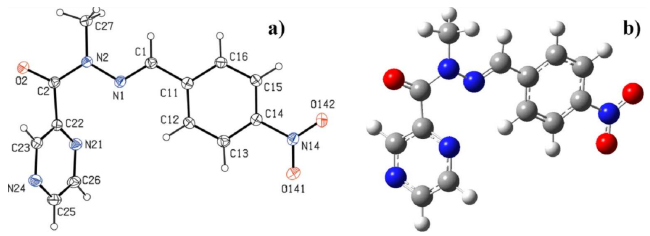

Fig. 1. (a) The experimental geometric structure [8], (b) optimized molecular structure (with B3LYP/6-311++G(d,p) level) of the title compound.

The title molecule belongs to the $C2/c$ space group. The unit cell dimensions are $a = 17.510(2)$ Å, $b = 10.5421(11)$ Å, $c = 14.9638(14)$ Å and $V = 2628.7(5)$ Å^3 and has eight formula units per unit cell ($Z = 8$). These results are taken from the data reported by Gomes et al. [8].

The optimized geometrical parameters (bond distances, bond angles and dihedral angles) are presented in Tables I–III and compared with the experimental X-ray diffraction [8] of a compound having similar structure. The correlation coefficient for the calculated and the experimental values of the molecule are shown in Tables.

The changes in the bond length of C–H bond on substitution due to a change in the charge distribution on the carbon atom of the benzene ring [28]. The carbon atoms are bonded to the hydrogen atoms with σ-bond in benzene and substitution of NO_2 group for hydrogen reduces the electron density at the ring carbon atom.

The bond length of N–O in nitro group is somewhat different and it is due to the repulsion between the lone electron pair on the O atom and the electron pair on the nitrogen atom [29]. In the present work, the C–H bond lengths were calculated in the range 1.0710–1.0939 Å, experimentally the C–H bond lengths are observed as 0.95 and 0.98 Å.

In substituted benzenes, the ring carbon atoms exert a large attraction on the valence electron cloud of the H atom resulting in an increase in the C–H force constant and a decrease in the corresponding bond length [30]. The C1–C11 and C2–C22 bond distances are the longest while the other C–C bond distances are shortest. The longest bond distance attributes the pure single bond character. In the benzene ring the C11–C12 bond length is slightly longer than C12–C13. The longest bond distance observed in the benzene ring is C11–C12.

TABLE I

The values of distances(Å) between atoms calculated for the title compound using B3LYP and HF methods compared with experimental data [8]

	Exp. [8]	Calc. B3LYP		Calc. HF	
	$A1$	$A2$	$A1$	$A2$	
O2-C2	1.224(2)	1.2160	1.2167	1.1912	1.1922
O141-N14	1.231(2)	1.2242	1.2254	1.1865	1.1874
O142-N14	1.225(2)	1.2244	1.2256	1.1869	1.1878
N1-C1	1.278(3)	1.2832	1.2835	1.2539	1.2543
N1-N2	1.379(2)	1.3519	1.3539	1.3467	1.3478
N2-C2	1.369(2)	1.3930	1.3910	1.3727	1.3711
N2-C27	1.458(2)	1.4607	1.4605	1.4505	1.4507
N14-C14	1.470(2)	1.4765	1.4760	1.4638	1.4648
N21-C22	1.337(2)	1.3353	1.3345	1.3158	1.3150
N21-C26	1.339(3)	1.3331	1.3333	1.3154	1.3157
N24-C25	1.336(3)	1.3349	1.3348	1.3163	1.3165
N24-C23	1.336(3)	1.3328	1.3326	1.3168	1.3164
C1-C11	1.470(3)	1.4651	1.4655	1.4784	1.4791
C1-H1	0.9500	1.0900	1.0899	1.0784	1.0786
C2-C22	1.512(3)	1.5073	1.5079	1.5067	1.5078
C11-C16	1.397(3)	1.4031	1.4035	1.3882	1.3886
C11-C12	1.402(3)	1.4059	1.4060	1.3941	1.3945
C12-C13	1.381(3)	1.3843	1.3849	1.3768	1.3775
C12-H12	0.9500	1.0819	1.0820	1.0721	1.0723
C13-C14	1.388(3)	1.3941	1.3949	1.3852	1.3857
C13-H13	0.9500	1.0810	1.0813	1.0711	1.0715
C14-C15	1.388(3)	1.3896	1.3903	1.3777	1.3779
C15-C16	1.389(3)	1.3883	1.3888	1.3834	1.3843
C15-H15	0.9500	1.0808	1.0811	1.0710	1.0714
C16-H16	0.9500	1.0845	1.0846	1.0752	1.0754
C22-C23	1.391(3)	1.3989	1.3986	1.3868	1.3872
C23-H23	0.9500	1.0845	1.0848	1.0736	1.0741
C25-C26	1.385(3)	1.3945	1.3948	1.3860	1.3864
C25-H25	0.9500	1.0859	1.0857	1.0753	1.0753
C26-H26	0.9500	1.0859	1.0857	1.0751	1.0751
C27-H27A	0.9800	1.0860	1.0863	1.0757	1.0761
C27-H27B	0.9800	1.0939	1.0938	1.0861	1.0860
C27-H27C	0.9800	1.0934	1.0933	1.0847	1.0847
R^2		0.9793	0.9799	0.9631	0.9633

The experimental C–N bond lengths fall in the range 1.278–1.470 Å and the optimized C–N bond lengths fall in the range 1.2835–1.4760 Å by B3LYP/6-311++G(d,p) method. From these values, a small difference between experimental and calculated bond lengths is observed.

The C12–C13–C14 and C14–C15–C16 ring angles are slightly smaller than 119° at the point substitution and longer than 119° at the other position, due to this reason the symmetry of the ring is slightly distorted. The rest of computed bond angles were correlated with the experimental values (see Table II). The highest correlation coefficient was obtained for DFT/B3LYP method with 6-311++G(d,p) basis set. In addition, this study concludes that the theoretically calculated dihedral angles are in good agreement with the experimental study [8].

TABLE II

The values of bond angles(°) calculated for the title compound using B3LYP and HF methods compared with experimental data [8]

	Exp. [8]	Calc. B3LYP		Calc. HF	
	*A*1	*A*2	*A*1	*A*2	
C1-N1-N2	117.97(16)	120.41	120.30	121.30	121.26
C2-N2-N1	116.92(15)	117.71	117.35	117.30	117.15
C2-N2-C27	120.87(15)	119.09	119.51	119.82	120.09
N1-N2-C27	122.20(15)	123.01	123.01	122.35	122.34
O142-N14-O141	123.44(17)	124.80	124.63	124.88	124.79
O142-N14-C14	118.25(16)	117.62	117.70	117.58	117.62
O141-N14-C14	118.30(16)	117.58	117.67	117.55	117.59
C22-N21-C26	115.43(17)	116.22	116.25	116.87	116.87
C25-N24-C23	115.58(17)	116.20	116.36	116.81	116.90
N1-C1-C11	119.52(17)	120.40	120.51	120.43	120.42
N1-C1-H1	120.2	123.18	123.08	123.43	123.41
C11-C1-H1	120.2	116.42	116.41	116.13	116.17
O2-C2-N2	121.95(17)	121.59	121.85	121.92	122.07
O2-C2-C22	119.60(17)	119.89	120.17	119.40	119.54
N2-C2-C22	118.44(16)	118.52	117.98	118.68	118.38
C16-C11-C12	119.38(17)	119.04	119.01	119.40	119.40
C16-C11-C1	118.91(17)	119.10	118.95	118.84	118.78
C12-C11-C1	121.66(17)	121.87	122.04	121.76	121.82
C13-C12-C11	120.53(17)	120.54	120.56	120.36	120.37
C13-C12-H12	119.7	120.57	120.38	120.24	120.14
C11-C12-H12	119.7	118.89	119.05	119.40	119.48
C12-C13-C14	118.41(18)	119.02	119.01	118.94	118.91
C12-C13-H13	120.8	121.72	121.52	121.23	121.15
C14-C13-H13	120.8	119.26	119.47	119.83	119.95
C13-C14-C15	122.98(18)	121.86	121.86	122.00	122.04
C13-C14-N14	118.50(17)	119.12	119.12	119.03	119.00
C15-C14-N14	118.52(17)	119.02	119.02	118.98	118.95
C14-C15-C16	117.64(17)	118.61	118.58	118.48	118.44
C14-C15-H15	121.2	119.49	119.72	120.14	120.26
C16-C15-H15	121.2	121.91	121.69	121.39	121.30
C15-C16-C11	121.04(18)	120.93	120.98	120.82	120.84
C15-C16-H16	119.5	119.38	119.33	119.15	119.12
C11-C16-H16	119.5	119.69	119.69	120.03	120.04
N21-C22-C23	122.45(17)	121.77	121.86	121.67	121.74
N21-C22-C2	119.39(16)	119.73	118.93	119.55	119.13
C23-C22-C2	117.89(16)	118.17	118.91	118.53	118.89
N24-C23-C22	121.90(17)	121.88	121.72	121.44	121.35
N24-C23-H23	119.0	117.60	117.56	117.82	117.84
C22-C23-H23	119.0	120.52	120.72	120.74	120.81
N24-C25-C26	122.57(19)	121.93	121.86	121.68	121.63
N24-C25-H25	118.7	117.07	117.18	117.42	117.51
C26-C25-H25	118.7	121.00	120.96	120.90	120.86
N21-C26-C25	122.05(18)	121.96	121.90	121.49	121.48
N21-C26-H26	119.0	116.97	117.06	117.41	117.48
C25-C26-H26	119.0	121.07	121.03		
N2-C27-H27A	109.5	107.31	107.54		
N2-C27-H27B	109.5	110.47	110.51		
H27A-C27-H27B	109.5	109.42	109.35	109.12	109.12
N2-C27-H27C	109.5	110.30	110.19	110.26	110.20
H27A-C27-H27C	109.5	109.92	109.76	109.41	109.33
H27B-C27-H27C	109.5	109.40	109.46	109.38	109.43
R^2		0.8963	0.9029	0.8964	0.8998

TABLE III

The values of dihedral angles(°) calculated for the title compound using B3LYP and HF methods compared with experimental data [8]

	Exp. [8]	Calc. B3LYP		Calc. HF	
	*A*1	*A*2	*A*1	*A*2	
C1-N1-N2-C2	178.94(16)	178.79	178.74	177.18	177.39
C1-N1-N2-C27	-0.1	3.94	-3.05	5.55	-4.77
N2-N1-C1-C11	-175.23	-179.75	-179.61	179.85	-179.72
N1-N2-C2-O2	178.58(16)	-167.45	168.47	164.70	165.92
C27-N2-C2-O2	-2.4	7.61	-7.38	7.15	-6.88
N1-N2-C2-C22	-0.8	13.25	-12.34	16.21	-14.93
C27-N2-C2-C22	178.22(15)	-171.68	171.82	171.94	172.27
N1-C1-C11-C16	-179.05	178.07	-178.16	177.61	-177.27
N1-C1-C11-C12	3.5(3)	-2.06	1.90	2.50	2.81
C16-C11-C12-C13	-1.3	-0.11	-0.13	0.11	-0.16
C1-C11-C12-C13	176.12(17)	-179.99	179.93	180.00	179.92
C11-C12-C13-C14	0.6(3)	-0.00	0.04	0.02	0.08
C12-C13-C14-C15	1.0(3)	0.10	0.07	0.05	0.02
C12-C13-C14-N14	-178.83	179.98	-179.97	179.96	-179.95
O142-N14-C14-C13	-173.56	179.90	-179.89	179.82	-179.83
O141-N14-C14-C13	6.8(3)	-0.10	0.11	0.19	0.18
O142-N14-C14-C15	6.6(3)	-0.23	0.20	0.27	0.24
O141-N14-C14-C15	-173.05	179.78	-179.80	179.72	-179.75
C13-C14-C15-C16	-1.8	-0.08	-0.07	0.04	-0.03
N14-C14-C15-C16	178.07(16)	-179.95	179.97	179.95	179.96
C14-C15-C16-C11	1.0(3)	-0.04	0.04	0.05	0.05
C12-C11-C16-C15	0.5(3)	0.14	0.13	0.12	0.14
C1-C11-C16-C15	-176.98	-179.99	-179.93	179.98	-179.94
C26-N21-C22-C23	-0.8	0.64	-0.39	0.42	-0.24
C26-N21-C22-C2	-174.73	174.01	-174.04	174.55	-174.59
O2-C2-C22-N21	118.3(2)	-130.59	122.81	130.07	125.14
N2-C2-C22-N21	-62.3	48.72	-56.40	49.04	-54.04
O2-C2-C22-C23	-55.9	43.01	-51.03	44.24	-49.38
N2-C2-C22-C23	123.49(19)	-137.68	129.76	136.65	131.45
C25-N24-C23-C22	-0.4	1.95	-1.86	1.81	-1.77
N21-C22-C23-N24	0.9(3)	-2.34	2.06	1.97	1.81
C2-C22-C23-N24	174.98(18)	-175.81	175.71	176.15	176.18
C23-N24-C25-C26	-0.3	-0.08	-0.20	0.29	-0.34
C22-N21-C26-C25	0.2(3)	1.22	1.28	1.10	1.20
N24-C25-C26-N21	0.4(4)	-1.58	1.44	1.23	1.21
R^2		0.9972	0.9986	0.9970	0.9981

3.2. NMR spectral analysis

Geometrical structures of studied compound were optimized by HF and DFT/B3LYP methods and the gauge-independent atomic orbital (GIAO) [31], the continuous set of gauge transformations (CSGT) [32] and the individual gauges for atoms in molecules (IGAIM, a slight variation on the CSGT method) [33] methods were used for prediction of nuclear shielding.

Theoretical and experimental chemical shifts of the title molecule in ^{1}H and ^{13}C NMR spectra in comparison with experimental chemical shifts are gathered in Table IV. The linear correlation between proton and carbon NMR shieldings of studied compound and experimental data is shown in Table IV. This data show good

TABLE IV

Experimental [8] and theoretical B3LYP and HF with 6-311++G(d,p) chemical shifts δ [ppm] of the title compound in ^{1}H and ^{13}C NMR spectra

	Exp. [8]	Calc. B3LYP			Calc. HF		
		GIAO	CSGT	IGAIM	GIAO	CSGT	IGAIM
^{1}H NMR ($CDCl_3$)							
H3	8.85	9.02	9.83	9.12	9.43	9.46	9.46
H5	8.70	8.76	9.58	8.86	9.15	9.23	9.22
H6	8.70	8.66	9.47	8.75	8.96	9.08	9.08
H3′	8.17	8.20	8.79	8.07	8.84	8.67	8.67
H5′	8.17	8.42	8.93	8.21	9.05	8.84	8.84
N=CH	7.84	7.53	8.60	7.88	7.69	7.99	7.99
H2′	7.52	7.66	8.54	7.83	8.02	8.19	8.19
H6′	7.52	7.30	8.22	7.50	7.72	7.91	7.91
NCH_3	3.64	5.14	5.98	5.26	5.04	5.26	5.26
NCH_3	3.64	2.72	3.98	3.27	2.92	3.48	3.48
NCH_3	3.64	2.56	3.82	3.10	2.69	3.24	3.24
R^2		0.9205	0.9360	0.9361	0.9357	0.9496	0.9496
^{13}C NMR							
C2	167.7	174.2	172.6	172.6	178.6	177.7	177.7
C22	149.8	157.4	155.1	155.0	160.9	158.6	158.6
C23	148.4	151.6	149.1	149.1	156.0	153.6	153.6
C25	145.2	150.5	148.6	148.6	155.4	153.7	153.7
C14	144.8	154.4	151.5	151.5	154.7	152.2	152.2
C11	143.8	147.0	146.6	146.6	154.3	153.8	153.8
C26	139.9	147.6	145.5	145.5	150.6	149.2	149.2
C1	138.1	137.9	137.6	137.6	141.9	142.0	142.0
C15	128.8	129.3	126.9	126.9	138.0	135.7	135.7
C13	128.8	129.3	127.0	127.0	137.8	135.6	135.6
C16	127.8	133.0	132.7	132.7	136.9	136.4	136.3
C12	124.2	128.8	127.4	127.4	133.9	132.6	132.6
C27	28.9	27.1	27.7	27.7	31.2	32.1	32.1
R^2		0.9939	0.9940	0.9940	0.9972	0.9975	0.9975

correlation between predicted and observed proton and carbon chemical shifts but the higher value of correlation coefficient was obtained by HF (CSGT and IGAIM) method (see supplementary information). The results are based on fixed geometry and a rigid conformation. Aromatic carbon atoms in benzene ring give signals in overlapped areas of the spectrum with chemical shift values from 120 to 160 ppm. The cumulative effect of nitrogen and oxygen reduce the electron density of the carbon atom C2, thus its NMR signal is observed in the very downfield at 167.7 ppm experimentally. This signal calculated in the range 172.6–178.6 ppm. ^{1}H chemical shifts were obtained by complete analysis of the NMR spectrum and interpreted critically to quantify different effects acting on the chemical shifts of protons. The hydrogen atoms in the benzene ring shows NMR peaks in the normal range of aromatic hydrogen atoms and are assigned to the chemical shift values 8.17 (H3', H5') and 7.52 (H2' and H6') ppm. The computed chemical shift values of 8.20–9.05 (H3', H5') and 7.30–8.54 (H2' and H6') ppm for proton atoms are in good agreement with the measured values (8.17 and 7.52 ppm).

3.3. Frontier molecular orbital analysis

The energies of four important molecular orbitals of the title molecule: the second highest and highest occupied MO's (HOMO and HOMO-1), the lowest and the second lowest unoccupied MO's (LUMO and LUMO+1) were calculated and are presented in Fig. 2 with the 3D plots. The energy gap of the title molecule was calculated at B3LYP/6-311++G(d,p) level, which reveals the chemical reactivity and proves the occurrence of eventual charge transfer.

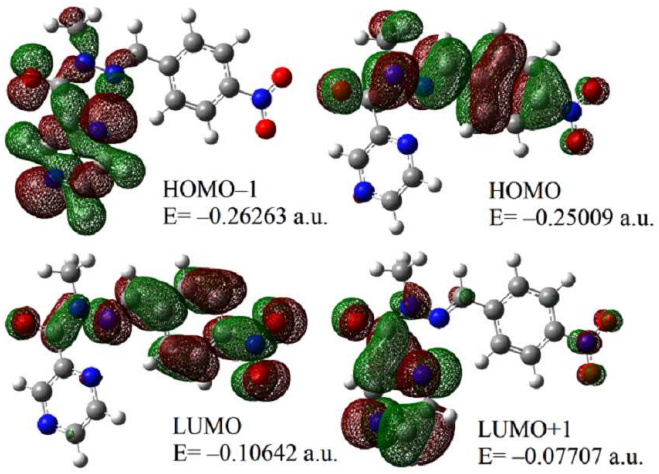

Fig. 2. The atomic orbital composition of the frontier molecular orbital of the title compound obtained by B3LYP/6-311++G(d,p) level.

The HOMO (ability to donate an electron) is located almost over the carbon atoms, oxygen atoms and also slightly delocalized in hydrogen atom and the LUMO (ability to obtain an electron) is mainly delocalized in carbon atoms of benzene ring and nitro group.

The energy gap (energy difference between HOMO and LUMO orbital) is a critical parameter in determining molecular electrical transport properties [34]. The HOMO–LUMO energy gap of the title molecule is found to be 0.14367 a.u. obtained at DFT/B3LYP method with 6-311++G(d,p) level. The energy gap also determines the chemical hardness softness of a molecule. By using the energies of the HOMO and LUMO orbitals, absolute hardness value of a molecule can be formulated by the equation: $\eta = (1/2)(-\varepsilon_{\mathrm{HOMO}} + \varepsilon_{\mathrm{LUMO}})$ [35–37]. The value of hardness is 0.071835 a.u. for the title molecule. Molecules having a large energy gap are known as hard and having a small energy gap are known as soft molecules. Soft molecules are more polarizable than hard molecules because they need small excitation energies to the manifold of excited states [38].

3.4. Potential energy surface scan

Visualizing and describing the relationship between potential energy and molecular geometry is called a potential energy surface (PES) that is an important to reveal

all possible conformations of the title molecule. The scan studies were obtained by minimizing the potential energy in all geometrical parameters by varying the torsion angle at a step of 10° in the range of 0–360° rotation around the bond. For the calculation, all the geometrical parameters were synchronically relaxed while the C1–N1–N2–C2 angle was varied in steps of 10°. The 2D surface in a 3D diagram and 2D surface countour graph of a PES scan performed for the dihedral angles C1–N1–N2–C2, N2–C2–C22–C23 and C1–N1–N2–C2, N1–C1–C11–C16 at the B3LYP/6-311G(d,p) level of theory for the title molecule is shown in Fig. 3 and Fig. 4.

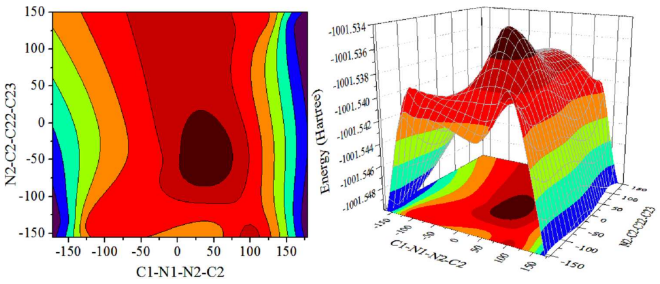

Fig. 3. PES reaction surface plot of C1–N1–N2–C2 and N2–C2–C22–C23 of the title compound obtained by B3LYP/6-311G(d,p) level.

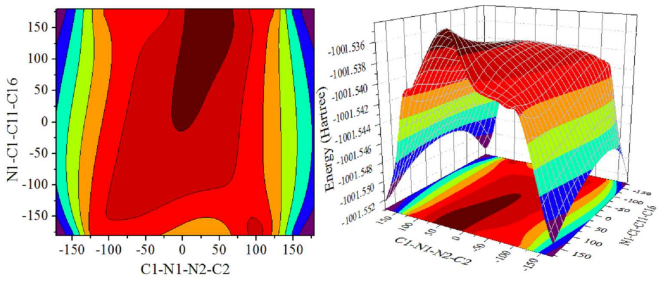

Fig. 4. PES reaction surface plot of C1–N1–N2–C2 and N1–C1–C11–C16 of the title compound obtained by B3LYP/6-311G(d,p) level.

The PES scan revealed that the C1–N1–N2–C2 dihedral angle has two energetically almost equal minimum energy at 179° with the energy of -1001.5521947200 and -1001.5521698000 Ha at a combination of N2–C2–C22–C23 dihedral angle of -138° and 137° and N1–C1–C11–C16 dihedral of −178° and 178°.

3.5. NPA and Mulliken atomic charges

The Mulliken analysis is the most popular population analysis method, it is by default always performed in Gaussian. The first involve a direct partitioning of the molecular wave function into atomic contributions following some arbitrary, orbital-based scheme proposed by Mulliken [39]. The Mulliken population analysis is one of the oldest and simplest, with the electrons being divided up amongst the atoms according to the degree to which different atomic AO basis functions contribute to the overall wave function [39]. The Mulliken charges do not achieve convergence with an increasing basis set size. Natural population analysis (NPA) and Mulliken methods predict the same tendencies.

The atomic charges of the title molecule acquired by the Mulliken population analysis and NPA with HF and B3LYP methods with 6-311G(d,p) and 6-311++G(d,p) basis sets are listed in Table V. The Mulliken and NPA atomic charges on each atom of the title compound are presented in the graphical representation shown in Fig. 5 and Fig. 6, respectively.

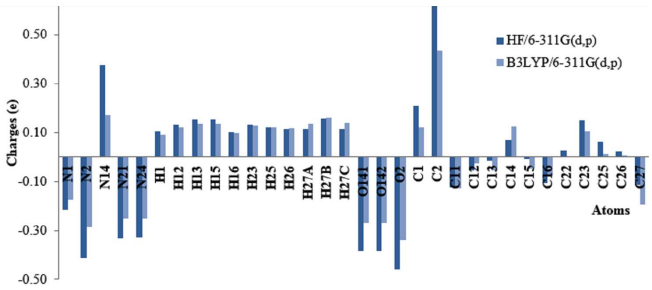

Fig. 5. Comparative Mulliken plot of the title compound obtained by HF and B3LYP methods with 6-311G(d,p) basis set.

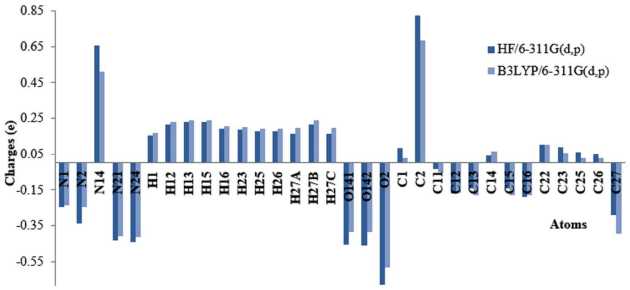

Fig. 6. Comparative NPA plot of the title compound obtained by HF and B3LYP methods with 6-311G(d,p) basis set.

From the results it is clear that carbon atoms attached with oxygen and nitrogen atoms are positive however the other carbon atoms have more negative charges. All hydrogen atoms have a positive charge and the oxygen and nitrogen atoms are negatively charged. The H13 and H15 atoms have positive and maximum atomic charges than the other hydrogen atoms. Due to the presence of electronegative oxygen atoms in the nitro group, nitrogen atom has large positive charge value N14. The methyl group nitrogen atom N2 has the maximum negative charge value compared to other nitrogen atoms of the nitro group N1, N21 and N24.

TABLE V

Calculated net charges by the Mulliken population analysis and NPA analysis of the title compound at B3LYP and HF methods with $A1$ and $A2$ basis sets

	Mulliken B3LYP		NPA B3LYP		Mulliken HF		NPA HF	
	$A1$	$A2$	$A1$	$A2$	$A1$	$A2$	$A1$	$A2$
N1	-0.17334	0.143948	-0.23435	-0.22274	-0.214765	0.223384	-0.24207	-0.24207
N2	-0.28705	0.128594	-0.24345	-0.27518	-0.413042	-0.027651	-0.33977	-0.33977
N14	0.171122	-0.215752	0.51253	0.49543	0.374672	-0.140153	0.65331	0.65331
N21	-0.251772	0.074446	-0.40773	-0.40048	-0.329997	0.063497	-0.42992	-0.42992
N24	-0.249485	-0.021276	-0.41098	-0.41385	-0.326651	-0.033727	-0.44156	-0.44156
H1	0.091974	0.14298	0.17003	0.17485	0.102714	0.188268	0.15529	0.15529
H12	0.120445	0.161184	0.22702	0.23397	0.131946	0.226894	0.21554	0.21554
H13	0.136977	0.251237	0.23848	0.24558	0.152037	0.294423	0.22790	0.22790
H15	0.136553	0.247044	0.23918	0.24649	0.151938	0.291166	0.22876	0.22876
H16	0.098834	0.169461	0.20693	0.21451	0.101861	0.208699	0.19376	0.19376
H23	0.129348	0.241297	0.19926	0.21214	0.132301	0.282065	0.18704	0.18704
H25	0.122332	0.202844	0.19023	0.20223	0.122813	0.232393	0.17563	0.17563
H26	0.116632	0.210304	0.19061	0.20119	0.116204	0.240658	0.17629	0.17629
H27A	0.13447	0.170014	0.19534	0.20361	0.113193	0.161593	0.16248	0.16248
H27B	0.159148	0.220229	0.23950	0.25700	0.158672	0.239811	0.21615	0.21615
H27C	0.137811	0.167767	0.19681	0.20445	0.114606	0.157342	0.16385	0.16385
O141	-0.268837	0.005985	-0.38394	-0.37908	-0.383066	-0.043376	-0.45676	-0.45676
O142	-0.26977	-0.003741	-0.38556	-0.38002	-0.384743	-0.053414	-0.45911	-0.45911
O2	-0.33721	-0.223964	-0.58049	-0.57941	-0.457382	-0.300768	-0.67880	-0.67880
C1	0.122074	-0.307487	0.02984	0.03017	0.209706	-0.350349	0.08229	0.08229
C2	0.433577	-0.637502	0.68295	0.67257	0.618384	-0.486406	0.82584	0.82584
C11	-0.127315	0.670062	-0.05334	-0.06810	-0.125833	0.590531	-0.03429	-0.03429
C12	-0.026036	-0.096548	-0.16675	-0.17279	-0.054627	-0.133537	-0.16802	-0.16802
C13	-0.053164	-0.459246	-0.17664	-0.18052	-0.015135	-0.490161	-0.14180	-0.14180
C14	0.124761	-0.209129	0.06402	0.06424	0.070462	-0.214371	0.04000	0.04000
C15	-0.047309	-0.246248	-0.17722	-0.18317	-0.00983	-0.26175	-0.13901	-0.13901
C16	-0.075744	-0.518585	-0.18075	-0.18320	-0.105093	-0.553734	-0.18741	-0.18741
C22	0.002056	0.052263	0.10319	0.09715	0.026507	-0.081208	0.10306	0.10306
C23	0.103368	-0.02367	0.05674	0.05420	0.150007	0.032641	0.09059	0.09059
C25	0.014236	-0.214642	0.02776	0.02309	0.06155	-0.258388	0.06235	0.06235
C26	0.004824	0.218781	0.02558	0.01615	0.02334	0.289192	0.04965	0.04965
C27	-0.193511	-0.300654	-0.39481	-0.41050	-0.112748	-0.293565	-0.29125	-0.29125

3.6. NBO analysis

The importance of the NBO method is originated from that it gives information about intra- and intermolecular bonding and interactions among bonds. Furthermore, it provides a convenient basis for investigating the interactions in both filled and virtual orbital spaces along with charge transfer and conjugative interactions in molecular system. The second-order Fock matrix was used to evaluate the donor acceptor interactions in the NBO basis [39]. The interactions result in a loss of occupancy from the localized NBO of the idealized Lewis structure into an empty non-Lewis orbital. For each donor (i) and acceptor (j), the stabilization energy E(2) associated with the delocalization $i \rightarrow j$ is estimated as [40]:

$$E\,(2) = \Delta E_{i \rightarrow j} = q_i \frac{F(i,j)^2}{(\varepsilon_j - \varepsilon_i)}, \tag{3.1}$$

where q_i is the donor orbital occupancy, ε_i and ε_j are the diagonal elements (orbital energies) and $F(i,j)$ is the off diagonal NBO Fock matrix element. The larger the $E(2)$ value, the more intensive is the interaction between electron donors and electron acceptors, i.e. the more donating tendency from electron donors to electron acceptors and the greater the extent of conjugation of the whole system [41].

NBO analysis has been performed on the molecule at the HF and DFT/B3LYP methods with 6-311++G(d,p) level in order to elucidate the possible donor–acceptor pairs, the values of the donor–acceptor stabilization energy as estimated by the above equation and NBO occupancies that are presented in Table VI. Tables also include the corresponding Fock matrix elements in the numerator and denominator of this equation.

The π electron delocalization is maximum around C23–N24, C25–C26 distributed to π^* antibonding of C25–C26, N21–C22 with a stabilization energy of about 50.03, 49.11 kcal/mol for HF/6-311++G(d,p) and 24.42, 20.35 kcal/mol for B3LYP/6-311++G(d,p). NBO analysis clearly manifests the evidences of the intramolecular charge transfer from σ(C27–H27A) to σ^*(N1–N2) antibonding orbitals that clearly shows that the hy-

droxyl group is inclined towards the $C27H_3$ group showing large stabilization energy of 6.94 kcal/mol (HF/6-311++G(d,p) and 5.69 kcal/mol (B3LYP/6-311++G(d,p). The most important interaction energies in this molecule are σ electron donating from LP(1)O141 $\rightarrow$ σ^*(C14 – N14) and LP (1) O141 $\rightarrow$ σ^*(C14–N14) resulting a stabilization energy of about 5.74, 4.20 kJ/mol respectively. In title molecule, the interaction of lone pair orbital on oxygen atom LP (3) O142 LP (3) O142 of the NBO conjugated with π^*(N14–O141) resulting to stabilization of 283.13 kcal/mol (HF) and 163.10 kcal/mol (B3LYP) shown in Table VI(at the end). Percentage of *s*, *p*, and *d*-character on each natural atomic hybrid of the natural bond orbital is listed in Table VII (at the end).

As shown in Table VI, the difference in polarization coefficients is small when similar atoms are involved in bond formation (C–C, N–N bond) however in C–N and C–O bond formations there are found considerable differences. The sizes of the polarization coefficients of the corresponding bond provides information about the electronegativity, the larger differences in the polarization coefficient values of the atoms involved in the bond formation are reflected in the electronegativity of the atoms.

4. Conclusion

The geometry of methylated pyrazine-2-carbohydrazide derivative, namely *N*-methyl-*N*′-(4-nitrobenzylidene)pyrazine-2-carbohydrazide was optimized at different levels with HF and DFT/B3LYP method using 6-311G(d,p) and 6-311++G(d,p). The computed geometries are benchmarks for predicting crystal structural data of the molecule. The calculated structural parameters (bond distances, bond angles and dihedral angles) compares well with the experimental values. The ^{1}H and ^{13}C NMR isotropic chemical shifts were calculated and the assignments made were compared with the experimental values. HOMO–LUMO gaps are examined and discussed. The potential energy curves have been obtained for C2–N2–N1–C1 and N1–C1–C11–C16 rotational angles at the same levels of theory. The NBO analysis revealed that the LP (3) O2 $\rightarrow$ LP* (1) C2 interaction gives the strongest stabilization to the system around at 416.19 kcal/mol with HF/6-311++G(d,p).

References

[1] A.K. Singh, P. Kumar, M. Yadav, D.S. Pandey, *J. Organomet. Chem.* **695**, 567 (2010).

[2] X.H. Zhao, S.S. Liu, Y.Z. Li, M.D. Chen, *Spectrochim. Acta A* **75**, 794 (2010).

[3] T. Asaki, T. Hamamoto, Y. Sugiyama, K. Kuwano, K. Kuwabara, *Bioorgan. Med. Chem.* **15**, 6692 (2007).

[4] J.W. Corbett, M.R. Rauckhorst, F. Qian, R.L. Hoffman, C.S. Knauer, L.W. Fitzgerald, *Bioorgan. Med. Chem.* **17**, 6250 (2007).

[5] H. Endredi, F. Billes, F.S. Holly, *J. Mol. Struct.* **633**, 73 (2003).

[6] S.R. Pattan, P.A. Rabara, J.S. Pattan, A.A. Bukitagar, V.S. Wakale, D.S. Musmade, *Indian J. Chem.* **48**, 1453 (2009).

[7] D. Sriram, P. Yogeeswari, S.P. Reddy, *Bioorgan. Med. Chem. Lett.* **16**, 2113 (2006).

[8] L.R. Gomes, J.N. Low, A.S.M.C. Rodrigues, J.L. Wardell, C.H. Lima, M.V.N. de Souza, *Acta Crystallogr. C* **69**, 549 (2013).

[9] S.M. Sondhi, M. Dinodia, A. Kumar, *Eur J. Med. Chem.* **44**, 1010 (2009).

[10] A. Tanitame, Y. Oyamada, K. Ofuji, H. Terauchi, M. Kawasaki, M. Wachi, J.-I. Yamagishi, *Bioorgan. Med. Chem. Lett.* **15**, 4299 (2005).

[11] I. Koca, A. Özgür, K.A. Coşkun, Y. Tutar, *Bioorgan. Med. Chem.* **21**, 3859 (2013).

[12] S. Tyagarajan, P.K. Chakravarty, B. Zhou, B. Taylor, R. Eid, M.H. Fisher, W.H. Parsons, M.J. Wyvratt, K.A. Lyons, T. Klatt, X. Li, S. Kumar, B. Williams, J. Felix, B.T. Priest, R.M. Brochu, V. Warren, M. Smith, M. Garcia, G.J. Kaczorowski, W.J. Martin, C. Abbadie, E. McGowan, N. Jochnowitz, A. Weber, J.L. Duffy, *Bioorgan. Med. Chem. Lett.* **20**, 7479 (2010).

[13] S.-R. Shih, T.-Y. Chu, G. Reddy, S.-N. Tseng, H.-L. Chen, W.-F. Tang, M.-S. Wu, J.-Y. Yeh, Y.-S. Chao, J.T.A. Hsu, H.-P. Hsieh, J.-T. Horng, *J. Biomed. Sci.* **17**, 13 (2010).

[14] H.Y. Lo, C.C. Man, R.W. Fleck, N.A. Farrow, R.H. Ingraham, A. Kukulka, J.R. Proudfoot, R. Betageri, T. Kirrane, U. Patel, R. Sharma, M.A. Hoermann, A. Kabcenell, S. de Lombaert, *Bioorgan. Med. Chem. Lett.* **26**, 6379 (2010).

[15] R. Kasimoğullari, M. Bülbül, B.S. Arslan, B. Gökçe, *Eur. J. Med. Chem.* **45**, 4769 (2010).

[16] A. Padmaja, C. Rajasekhar, A. Muralikrishna, V. Padmavathi, *Eur. J. Med. Chem.* **46**, 5034 (2011).

[17] N. Gökhan-Kelekçi, S. Koyunoglu, S. Yabanoglu, K. Yelekçi, Ö. Özgen, G. Uçar, K. Erol, E. Kendi, A. Yeşilada, *Bioorgan. Med. Chem.* **17**, 675 (2009).

[18] D.M. Shen, E.J. Brady, M.R. Candelore, Q. Dallas-Yang, V.D.-H. Ding, W.P. Feeney, G. Jiang, M.E. McCann, S. Mock, S.A. Qureshi, R. Saperstein, X. Shen, X. Tong, L.M. Tota, M.J. Wright, X. Yang, S. Zheng, K.T. Chapman, B.B. Zhang, J.R. Tata, E.R. Parmee, *Bioorgan. Med. Chem. Lett.* **21**, 76 (2011).

[19] K. Gobis, H. Foks, Z. Zwolska, E. Augustynowicz-Kopeć, *Heterocycles* **81**, 917 (2010).

[20] S.M.S.V. Wardell, M.V.N. de Souza, J.L. Wardell, J.N. Low, C. Glidewell, *Acta Crystallogr. E* **62**, 3765 (2006).

[21] M. Yoshida, T. Shimada, T. Ishida, T. Kogane, *Polyhedron* **66**, 75 (2013).

[22] B. Milczarska, K. Gobis, H. Foks, L. Golunski, P. Sowinski, *J. Heterocyclic Chem.* **49**, 845 (2012).

[23] A.D. Becke, *J. Chem. Phys.* **98**, 5648 (1993).

[24] C. Lee, W. Yang, R.G. Parr, *Phys. Rev. B* **37**, 785 (1988).

[25] M.J. Frisch, G.W. Trucks, H.B. Schlegel, G.E. Scuseria, M.A. Robb, J.R. Cheeseman, G. Scalmani, V. Barone, B. Mennucci, G.A. Petersson, H. Nakatsuji, M. Caricato, X. Li, H.P. Hratchian, A.F. Izmaylov, J. Bloino, G. Zheng, J.L. Sonnenberg, M. Hada, M. Ehara, K. Toyota, R. Fukuda, J. Hasegawa, M. Ishida, T. Nakajima, Y. Honda, O. Kitao, H. Nakai, T. Vreven, J.A. Montgomery Jr., J.E. Peralta, F. Ogliaro, M. Bearpark, J.J. Heyd, E. Brothers, K.N. Kudin, V.N. Staroverov, R. Kobayashi, J. Normand, K. Raghavachari, A. Rendell, J.C. Burant, S.S. Iyengar, J. Tomasi, M. Cossi, N. Rega, J.M. Millam, M. Klene, J.E. Knox, J.B. Cross, V. Bakken, C. Adamo, J. Jaramillo, R. Gomperts, R.E. Stratmann, O. Yazyev, A.J. Austin, R. Cammi, C. Pomelli, J.W. Ochterski, R.L. Martin, K. Morokuma, V.G. Zakrzewski, G.A. Voth, P. Salvador, J.J. Dannenberg, S. Dapprich, A.D. Daniels, Ö. Farkas, J.B. Foresman, J.V. Ortiz, J. Cioslowski, D.J. Fox, Gaussian 09, Revision A.1, Gaussian Inc., Wallingford CT, 2009.

[26] R. Dennington, T. Keith, J. Millam, Semichem Inc., Shawnee Mission KS, GaussView, Version 5, 2009.

[27] E.D. Glendening, A.E. Reed, J.E. Carpenter, F. Weinhold, NBO version 3.1.

[28] H. Pir, N. Gunay, Ö. Tamer, D. Avci, E. Tarcan, Y. Atalay, *Mater. Sci.-Poland* **31**, 357 (2013).

[29] Ö. Tamer, D. Avci, Y. Atalay, *Spectrochim. Acta A* **117**, 78 (2014).

[30] A. Kunduracioğlu, Ö. Tamer, D. Avci, İ. Kani, Y. Atalay, B. Çetinkaya, *Spectrochim. Acta A* **121**, 35 (2014).

[31] R. Ditchfield, *J.'Chem. Phys.* **56**, 5688 (1972).

[32] T.A. Keith, R.F.W. Bader, *Chem. Phys. Lett.* **210**, 223 (1993).

[33] T.A. Keith, R.F.W. Bader, *Chem. Phys. Lett.* **194**, 1 (1992).

[34] K. Fukui, *Science* **218**, 747 (1982).

[35] R.G. Parr, R.G. Pearson, *J. Am. Chem. Soc.* **105**, 7512 (1983).

[36] Ö. Tamer, N. Dege, G. Demirtaş, D. Avci, Y. Atalay, M. Macit, A. Alaman Agar, *Spectrochim. Acta A* **117**, 13 (2014).

[37] N. Dege, N. Şenyüz, H. Bati, N. Günay, D. Avci, Ö. Tamer, Y. Atalay, *Spectrochim. Acta A* **120**, 323 (2014).

[38] R.G. Pearson, *Proc. Natl. Acad. Sci.* **83**, 8440 (1986).

[39] A.E. Reed, L.A. Curtiss, F. Weinhold, *Chem. Rev.* **88**, 899 (1988).

[40] D.G. Truhlar, *J. Chem. Phys.* **82**, 2418 (1985).

[41] S. Sebastian, N. Sundaraganesan, *Spectrochim. Acta A* **75**, 941 (2010).

TABLE VI

Second order perturbation theory analysis of Fock matrix in NBO basis for the title compound at B3LYP and HF methods with $A2$ basis set

				B3LYP					HF				
Donor	Type	Acceptor	Type	Occup.		$E(2)$	$\Delta E(ji)$	$F(i.j)$	Occup.		$E(2)$	$\Delta E(ji)$	$F(i.j)$
(i)	(j)	(i) $[e]$	(j) $[e]$	$[\frac{\text{kcal}}{mol}]$	[a.u.]	[a.u.]	(i) $[e]$	(j) $[e]$	$[\frac{\text{kcal}}{mol}]$	[a.u.]	[a.u.]		
C25-C26	π	N21-C22	π^*	1.58507	0.38596	20.35	0.27	0.07	1.58005	0.37835	49.11	0.47	0.14
		C23-N24	π		0.33769	18.72	0.27	0.07		0.33643	43.01	0.48	0.13
C27–H27A	σ^*	N1-N2	σ^*	1.98492	0.03170	5.69	0.91	0.06	1.98857	0.02425	6.94	1.40	0.09
C2-C22	σ^*	N2-C27	σ^*	1.97278	0.03803	4.00	0.98	0.06	1.97492	0.02683	4.96	1.47	0.08
		N21-C26	σ^*		0.01510	3.44	1.20	0.06		0.01262	4.29	1.72	0.08
C22-C23	σ^*	N21-C22	σ^*						1.98481	0.01915	3.76	1.82	0.07
N21-C22	σ^*	C22-C23	σ^*						1.98397	0.03304	3.46	1.96	0.07
N21-C22	π	C25-C26	π^*	1.69569	0.28235	23.26	0.32	0.08	1.70090	0.28744	45.38	0.56	0.14
		C23-N24	π		0.33769	18.24	0.31	0.07		0.33643	37.03	0.55	0.13
		C2-O2	π		0.25039	6.66	0.34	0.04					
		LP*(1) C2								0.68128	10.51	0.38	0.06
C2-N2	σ^*	N1-C1	σ^*						1.98877	0.00835	3.22	2.03	0.07
N1-C1	π	C11-C12	π^*	1.91919	0.37085	8.63	0.37	0.05	1.94959	0.35442	10.97	0.64	0.08
C1-C11	σ^*	N1-N2	σ^*	1.97229	0.03170	4.70	1.05	0.06	1.97446	0.02425	6.25	1.57	0.09
		N1-C1	σ^*							0.00835	3.91	1.82	0.08
		C11-C12	σ^*							0.02243	3.00	1.72	0.06
C23-N24	π	C25-C26	π^*	1.69188	0.28235	24.42	0.32	0.08	1.68799	0.28744	50.03	0.55	0.15
		N21-C22	π		0.38596	18.42	0.31	0.07		0.37835	37.45	0.54	0.13
N21-C26	σ^*	C2-C22	σ^*	1.98455	0.07317	3.48	1.23	0.06	1.98599	0.06166	4.19	1.77	0.08
N14-O141	π	N14-O141	π^*	1.98566	0.62694	7.59	0.32	0.05	1.98949	0.53634	6.00	0.62	0.06
		C13-C14	π		0.39660	3.14	0.46	0.04					
		LP(3) O142		1.45055	12.37	0.18	0.08						
LP(1) N2		C27-H27A	σ^*	1.60569	0.01233	4.68	0.66	0.06	1.70789	0.01172	7.22	1.02	0.08
		C27-H27B	σ^*		0.01202	4.46	0.66	0.05		0.01089	6.38	1.02	0.08
		N1-C1	π^*		0.21554	33.57	0.28	0.09		0.13616	42.86	0.58	0.15
		C2-O2	π^*		0.25039	43.34	0.30	0.11					
		LP*(1) C2								0.68128	115.83	0.37	0.21
LP(2) O2		C2-C22	σ^*	1.85710	0.07317	18.84	0.66	0.10	1.89097	0.06166	26.28	1.09	0.15
		C2-N2	σ^*		0.08850	25.88	0.67	0.12		0.06794	35.23	1.16	0.18
LP(3) O2		LP*(1) C2							1.50115	0.68128	416.19	0.31	0.33
LP(1) N1		N2-C27	σ^*	1.91375	0.03803	10.66	0.70	0.08	1.93399	0.02683	12.49	1.17	0.11
		C1-C11	σ^*							0.02517	4.21	1.29	0.07
		C1-H1	σ^*		0.03353	10.65	0.78	0.08		0.02589	14.49	1.21	0.12
LP(1) N21		C25-C26	σ^*	1.91779	0.03375	8.28	0.91	0.08	1.93419	0.02807	10.57	1.37	0.11
		C2-C22	σ^*		0.07317	3.05	0.75	0.04		0.06166	4.91	1.19	0.07
		C22-C23	σ^*		0.04005	9.42	0.90	0.08		0.03304	12.13	1.37	0.12
		C26-H26	σ^*		0.02360	3.85	0.78	0.05		0.01913	6.17	1.22	0.08
LP(1) N24		C25-H25	σ^*	1.91886	0.02350	3.80	0.78	0.05	1.93515	0.01921	6.12	1.22	0.08
		C25-C26	σ^*		0.03375	8.40	0.90	0.08		0.02807	10.82	1.37	0.11
		C22-C23	σ^*		0.04005	8.63	0.90	0.08		0.03304	10.93	1.37	0.11
		C23-H23	σ^*		0.02349	3.76	0.78	0.05		0.01889	6.04	1.22	0.08
LP(1) O141		C14-N14	σ^*	1.98173	0.10477	4.20	1.07	0.06	1.98190	0.08316	5.74	1.59	0.09
LP(2) O141		C14-N14	σ^*	1.89976		12.21	0.56	0.07	1.92240		17.22	1.01	0.12
		N14-O142	σ^*		0.05483	18.95	0.72	0.11		0.04061	25.66	1.30	0.17
LP(1) O142		C14-N14	σ^*	1.98174	0.10477	4.20	1.07	0.06	1.98192	0.08316	5.74	1.59	0.09
LP(2) O142		C14-N14	σ^*	1.89971		12.22	0.56	0.07	1.92231		17.24	1.01	0.12
		N14-O141	σ^*		0.05472	18.92	0.72	0.11		0.04055	25.63	1.30	0.17
LP(3) O142		N14-O141	π^*	1.45055		163.10	0.14	0.14	1.50191	0.53634	283.13	0.35	0.29

$E(2)$ means energy of hyperconjugative interactions(stabilization energy). $\Delta E(ji)$ means energy difference between donor and acceptor i and j NBO orbitals. $F(i,j)$ is the Fock matrix element between i and j NBO orbitals.

TABLE VII

Hybrid compositions of the title compound at B3LYP and HF methods with 6-311++G(d,p) basis set

			B3LYP					HF				
Bond	Type	Atom	Occup.	s [%]	p [%]	d [%]	NBO	Occup.	s [%]	p [%]	d [%]	NBO
C25-C26	σ	C25	49.90	37.78	62.17	0.05	$0.7064(sp^{1.65})+0.7078(sp^{1.64})$	49.91	37.62	62.28	0.10	$0.7065(sp^{1.66})+0.7077(sp^{1.65})$
		C26	50.10	37.93	62.03	0.05		50.09	37.75	62.15	0.10	
C25-C26	σ^*	C25	50.10	37.78	62.17	0.05	$0.7078(sp^{1.65})-7.064(sp^{1.64})$	50.09	37.62	62.28	0.10	$0.7077(sp^{1.66})-0.7065(sp^{1.65})$
		C26	49.90	37.93	62.03	0.05		49.91	37.75	62.15	0.10	
C25-C26	π	C25	49.67	0.00	99.94	0.06	$0.7048(p)+0.7094(p)$	49.22	0.00	99.89	0.11	$0.7015(p)+0.7126(p)$
		C26	50.33	0.00	99.94	0.06		50.78	0.00	99.90	0.10	
C25-C26	π	C25	50.33	0.00	99.94	0.06	$0.7094(p)-7.048(p)$	50.78	0.00	99.89	0.11	$0.7126(p)-0.7015(p)$
		C26	49.67	0.00	99.94	0.06		49.22	0.00	99.90	0.10	
C25-N24	σ	C25	40.81	31.77	68.13	0.10	$0.6388(sp^{2.14})+0.7693(sp^{1.84})$	40.46	32.00	67.84	0.17	$0.6361(sp^{2.12})+0.7716(sp^{1.72})$
		N24	59.19	35.23	64.69	0.09		59.54	36.67	63.20	0.14	
C25-N24	σ^*	C25	59.19	31.77	68.13	0.10	$0.7693(sp^{2.14})-0.6388(sp^{1.84})$	59.54	32.00	67.84	0.17	$0.7716(sp^{2.12})-0.6361(sp^{1.72})$
		N24	40.81	35.23	64.69	0.09		40.46	36.67	63.20	0.14	
C22-N21	σ	C22	41.52	31.79	68.11	0.09	$0.6443(sp^{2.14})+0.7647(sp^{1.8})$	41.17	32.00	67.85	0.15	$0.6417(sp^{2.12})+0.7670(sp^{1.70})$
		N21	58.48	35.64	64.28	0.08		58.83	37.03	62.84	0.13	
C22-N21	σ^*	C22	58.48	31.79	68.11	0.09	$0.7647(sp^{2.14})-0.6443(sp^{1.8})$	58.83	32.00	67.85	0.15	$0.7670(sp^{2.12})-0.6417(sp^{1.70})$
		N21	41.52	35.64	64.28	0.08		41.17	37.03	62.84	0.13	
C22-N21	π	C22	44.32	0.00	99.90	0.10	$0.6657(p)+0.7462(p)$	45.05	0.00	99.86	0.14	$0.6712(p)+0.7413(p)$
		N21	55.68	0.01	99.83	0.15		54.95	0.01	99.79	0.21	
C22-N21	π	C22	55.68	0.00	99.90	0.10	$0.7462(p)-0.6657(p)$	54.95	0.00	99.86	0.14	$0.7413(p)-0.6712(p)$
		N21	44.32	0.01	99.83	0.15		45.05	0.01	99.79	0.21	
C2-N2	σ	C2	36.50	30.78	69.11	0.11	$0.6042(sp^{2.25})+0.7969(sp^{1.8})$	36.17	31.28	68.52	0.20	$0.6014(sp^{2.19})+0.7990(sp^{1.78})$
		N2	63.50	35.68	64.28	0.04		63.83	35.91	64.01	0.08	
C2-N2	σ^*	C2	63.50	30.78	69.11	0.11	$0.7969(sp^{2.25})-0.6042(sp^{1.8})$	63.83	31.28	68.52	0.20	$0.7990(sp^{2.19})-0.6014(sp^{1.78})$
		N2	36.50	35.68	64.28	0.04		36.17	35.91	64.01	0.08	
C2-O2	σ	C2	35.41	31.76	68.07	0.17	$0.595(sp^{2.14})+0.8037(sp^{1.54})$	35.03	33.01	66.76	0.24	$0.5919(sp^{2.02})+0.8060(sp^{1.30})$
		O2	64.59	39.39	60.49	0.12		64.97	43.46	56.39	0.15	
C2-O2	σ^*	C2	64.59	31.76	68.07	0.17	$0.8037(sp^{2.14})-0.595(sp^{1.54})$	64.97	33.01	66.76	0.24	$0.8060(sp^{2.02})-0.5919(sp^{1.30})$
		O2	35.41	39.39	60.49	0.12		35.03	43.46	56.39	0.15	
C2-O2	π	C2	30.99	0.92	98.63	0.45	$0.5567(p)+0.8307(p)$					
		O2	69.01	1.02	98.86	0.12						
C2-O2	π	C2	69.01	0.92	98.63	0.45	$0.8307(p)-0.5567(p)$					
		O2	30.99	1.02	98.86	0.12						
N2-C27	σ	N2	63.69	34.15	65.83	0.03	$0.798(sp^{1.93})+0.6026(sp^{3.44})$	64.38	34.36	65.58	0.05	$0.8024(sp^{1.91})+0.5968(sp^{3.35})$
		C27	36.31	22.49	77.37	0.14		35.62	22.91	76.84	0.25	
N2-C27	σ^*	N2	36.31	34.15	65.83	0.03	$0.6026(sp^{1.93})-0.798(sp^{3.44})$	35.62	34.36	65.58	0.05	$0.5968(sp^{1.91})-0.8024(sp^{3.35})$
		C27	63.69	22.49	77.37	0.14		64.38	22.91	76.84	0.25	
N2-N1	σ	N2	53.55	30.09	69.83	0.08	$0.7317(sp^{2.32})+0.6816(sp^{2.99})$	53.07	29.49	70.39	0.13	$0.7285(sp^{2.39})+0.6850(sp^{2.85})$
		N1	46.45	25.06	74.81	0.13		46.93	25.90	73.91	0.19	
N2-N1	σ^*	N2	46.45	30.09	69.83	0.08	$0.6816(sp^{2.32})-0.7317(sp^{2.99})$	46.93	29.49	70.39	0.13	$0.6850(sp^{2.39})-0.7285(sp^{2.85})$
		N1	53.55	25.06	74.81	0.13		53.07	25.90	73.91	0.19	
N14-O141	σ	N14	49.12	31.94	67.92	0.13	$0.7009(sp^{2.13})+0.7133(sp^{3.03})$	48.95	32.34	67.36	0.30	$0.6997(sp^{2.08})+0.7145(sp^{2.57})$
		O141	50.88	24.76	75.09	0.14		51.05	27.96	71.93	0.11	
N14-O141	σ^*	N14	50.88	31.94	67.92	0.13	$0.7133(sp^{2.13})-0.7009(sp^{3.03})$	51.05	32.34	67.36	0.30	$0.7145(sp^{2.08})-0.6997(sp^{2.57})$
		O141	49.12	24.76	75.09	0.14		48.95	27.96	71.93	0.11	
N14-O141	π	N14	39.55	0.00	99.75	0.25	$0.6289(p)+0.7775(p)$	33.78	0.00	99.44	0.56	$0.5812(p)+0.8138(p)$
		O141	60.45	0.00	99.86	0.14		66.22	0.00	99.87	0.13	
N14-O141	π	N14	60.45	0.00	99.75	0.25	$0.7775(p)-0.6289(p)$	66.22	0.00	99.44	0.56	$0.8138(p)-0.5812(p)$
		O141	39.55	0.00	99.86	0.14		33.78	0.00	99.87	0.13	
N14-O142	σ	N14	49.12	31.95	67.92	0.13	$0.7009(sp^{2.13})+0.7133(sp^{3.03})$	48.97	32.34	67.36	0.30	$0.6998(sp^{2.08})+0.7144(sp^{2.58})$
		O142	50.88	24.75	75.11	0.14		51.03	27.93	71.96	0.11	
N14-O142	σ^*	N14	50.88	31.95	67.92	0.13	$0.7133(sp^{2.13})-0.7009(sp^{3.03})$	51.03	32.34	67.36	0.30	$0.7144(sp^{2.08})-0.6998(sp^{2.58})$
		O142	49.12	24.75	75.11	0.14		48.97	27.93	71.96	0.11	